ISSN 0040-5795, Theoretical Foundations of Chemical Engineering, 2020, Vol. 54, No. 4, pp. 655–663. © Pleiades Publishing, Ltd., 2020.

Low-Cost Magnetic Fe_3O_4/Chitosan Nanocomposites for Adsorptive Removal of Carcinogenic Diazo Dye

Avinash Kadam[a, b], Jiseon Jang[b, c], Seong-Rin Lim[d, *], and Dae Sung Lee[b, **]

[a]Research Institute of Biotechnology and Medical Converged Science, Dongguk University, Biomedi Campus, Ilsandong-gu, Goyang-si, Gyeonggi-do, 10326 Republic of Korea

[b]Department of Environmental Engineering, Kyungpook National University, Buk-gu, Daegu, 41566 Republic of Korea

[c]R&D Institute of Radioactive Wastes, Korea Radioactive Waste Agency, 174 Gajeong-ro, Yuseong-gu, Daejeon, 34129 Republic of Korea

[d]Department of Environmental Engineering, Kangwon National University, Chuncheon, Gangwon, 24341 Republic of Korea

*e-mail: srlim@kangwon.ac.kr

**e-mail: daesung@knu.ac.kr

Received March 22, 2017; revised February 26, 2018; accepted March 6, 2018

Abstract—The eco-friendly adsorptive removal of Congo red (CR) from aqueous medium using Fe_3O_4/chitosan nanocomposites was investigated. The nanocomposites were synthesized by using a cost effective reductive precipitation method. The structural characterization of nanocomposties was determined by field emission scanning electron microscopy, thermal gravimetric analysis, fourier transform infrared spectroscopy, and magnetic property measurement system. Successful coating of chitosan on the iron oxide nanoparticles was confirmed by field emission scanning electron microscopy. The synthesized nanocomposites showed a maximum adsorption capacity of 47 mg/g for CR from an aqueous solution. Based on non-linear regression, the Langmuir isotherm fitted the experimental data better than the Freundlich and Tempkin models. The separation factor (R_L) calculated from the Langmuir adsorption isotherm indicated that CR adsorption on the nanocomposites was favorable. The obtained Fe_3O_4/chitosan nanocomposite is a cost-effective adsorbent and can be easily retrieved from an aqueous solution by a magnet after decontamination of CR.

Keywords: Congo red, magnetic nanoparticles, chitosan, adsorption, reduction precipitation method

DOI: 10.1134/S0040579520040193

INTRODUCTION

Textile dyes are recognized as one of the larger groups of pollutants in the wastewater released from several industries [1]. Textile wastewater released into the environment is highly hazardous to aquatic flora and fauna [2]. Congo red (CR; 3'-([1,1'-biphenyl]-4,4'-diyl)bis(4-aminonaphthalene-1-sulfonic acid) disodium salt] is a diazo benzidine-based anionic textile dye. The complex aromatic structure of CR makes biodegradation of this compound difficult. The structure of CR contains a benzidine moiety, and CR is known to be a potent human carcinogen [3]. Due to these deleterious health impacts, CR is banned in many countries, even though it is still extensively used in some of the developing countries. Thus, removal of CR from aqueous systems is a vital undertaking for environmental sustainability [2].

Adsorption is a low cost and economical technique for treatment of wastewater containing textile dyes [4, 5]. Different adsorbents such as alumina and bauxite, silica gel, zeolites, and activated carbons have been proposed for wastewater treatment, where low cost waste materials are particularly attractive for this purpose [6]. Recently, the exploitation of natural biopolymer materials as adsorbents for wastewater treatment has attracted remarkable interest. Specifically, chitosan (a cationic polymer) and its derivatives have been brought into the spotlight [7]. Chitosan is an abundant natural biopolymer isolated from the exoskeleton of crustaceans [8]. Chitosan mainly contains β-1 → 4 linked 2-amino-2-deoxy-glucopyranose (GlcN) and 2-acetamido-2-deoxy-β-D-glucopyranose (GlcNAc) residues, and is commercially manufactured on a large scale via alkaline *N*-deacetylation of chitin [7]. The high content of adsorptive amino ($-NH_2$) and hydroxyl ($-OH$) groups in chitosan makes it useful as an adsorbent for purification of wastewater containing anionic dyes, heavy metals, and radionuclides [9].

It is generally very difficult to separate the used adsorbents (containing pollutants on their surface) from treated wastewater subsequent to the adsorption process [10]. In order to tackle this problem during wastewater treatment, a suitable separation technique must be employed. Hence, incorporation of magnetic characteristics into the adsorbent materials is one

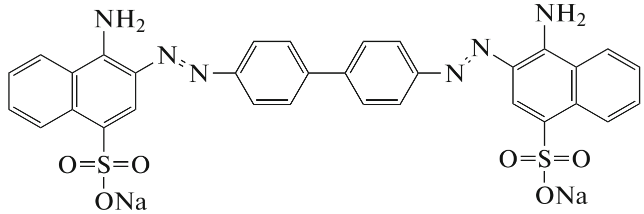

Fig. 1. Molecular structure of CR [1-naphthalene sulfonic acid, 3,30-(4,40-biphenylenebis(azo))bis(4-amino-)disodium salt].

approach for enhancing the value of these adsorbents as water/wastewater purification materials [10]. Magnetic nano-adsorbents are used for removal of pollutants from wastewater via surface adsorption and can be subsequently separated by simple application of a magnetic force [11].

Recently, Fe_3O_4/chitosan nanomaterials, in which chitosan serves as an efficient adsorbent containing a dispersed phase of magnetic iron oxide (Fe_3O_4) particles, were found to be strikingly effective materials for wastewater treatment [10]. Among the natural biopolymers that have been evaluated as engineering magnetic materials, chitosan is frequently employed as a base material due to its notable features of biodegradability, biocompatibility, availability, cost effectiveness, low cytotoxicity, chemical properties, and versatility [12–15]. A low cost reduction precipitation method has been used for synthesis of Fe_3O_4/chitosan nanocomposites [16]. Additional modifications to this process such as incorporation of a nontoxic cross-linking agent, glutaraldehyde, and the use of room temperature conditions for mixing would make the process more economical [17]. Hence, the use of a distinctive and inexpensive nano-adsorbent with high adsorption efficiency and magnetic properties to enable separation of CR from aqueous media should facilitate economical and ecofriendly treatment of wastewater.

The objective of this work is to the synthesis of Fe_3O_4/chitosan nanocomposites for the adsorptive removal of CR by low cost reduction precipitation method. Detailed characterization of the Fe_3O_4/chitosan nanocomposites is carried out by using techniques such as field emission scanning electron microscopy (FE-SEM), thermal gravimetric analysis (TGA), fourier transform infrared spectroscopy (FT-IR) and magnetic property measurement system (MPMS). The dynamics of isothermal adsorption of CR on Fe_3O_4/chitosan are studied using Langmuir, Freundlich, and Tempkin models.

EXPERIMENTAL

Materials. All chemicals used herein were of analytical grade, the highest purity available. The textile dye CR, ethyl alcohol, acetone, and ferric chloride were obtained from Dae-Jung (South Korea). Sodium sulfite was received from Junsei (South Korea). Chitosan (93% deacetylation) was purchased from Sigma-Aldrich (USA). The molecular structure of CR is presented in Fig. 1.

Synthesis. In the typical synthesis process, 70 mL of 0.1 N HCl solution containing $FeCl_3$ (2–2.45 g) and 50 mL of 1% HCl containing chitosan (0.5–1 g) were mixed. This mixture was stirred continuously for 1 h. Na_2SO_3 solution (0.720 g in 30 mL) was added to the mixture. The initially yellow colored mixture turned red after this addition. When the red mixture became yellow again, 50 mL of ammonia solution (12%) was instantly added with vigorous stirring. A black colored precipitate was formed after addition of the ammonia solution. The cross-linking agent glutaraldehyde (5 mL) was immediately added to the mixture that was then continuously stirred for 2 h at room temperature. The obtained black precipitate was separated with the aid of an adscititious magnet. This black precipitate was washed several times in sequence with distilled water, absolute ethanol, and acetone. The same procedure was used for iron oxide (Fe_3O_4) synthesis, except for the addition of chitosan and glutaraldehyde. Finally, the obtained precipitate was dried in a vacuum oven at a 60°C overnight. The obtained composites were ground to a fine powder for further use.

Characterization. The nanostructures of the synthesized Fe_3O_4/chitosan nanocomposites were studied by using field emission scanning electron microscopy (FE-SEM, Hitachi S-4800). Thermogravimetric analysis (TGA) was carried out from room temperature to 800°C at a heating rate of 10°C/min under a nitrogen atmosphere by using a thermal analyzer system (TA Instrument, Q600). Fourier transform infrared spectroscopy (FT-IR) data were acquired by using an infrared spectrometer (Perkin Elmer, Fontier). The supermagnetic properties of the sample were analyzed by a SQUID-VSM QM02 magnetometer at room temperature with an applied field between –15.000 and 15.000 Oe.

Adsorption experiment. Adsorption experiments were carried out using a batch scale process. In a representative process, Fe_3O_4/chitosan nanocomposites (1 g/L) were added to a 25 mL solution of CR (50 mg/L) at pH 3.0. The obtained mixture was stirred for 24 h at 140 rpm at a temperature of 30°C. After the adsorption process, the adsorbents were removed by using an adscititious magnet; the absorption of the resulting solution was measured at the maximum absorption wavelength of CR (λ_{max}: 500 nm) using a UV-vis spectrophotometer (Agilent 8453). The adsorption capacity, q_e (mg/g), was determined by means of the following equation:

$$q_e = \frac{(C_0 - C_e)V}{W}, \tag{1}$$

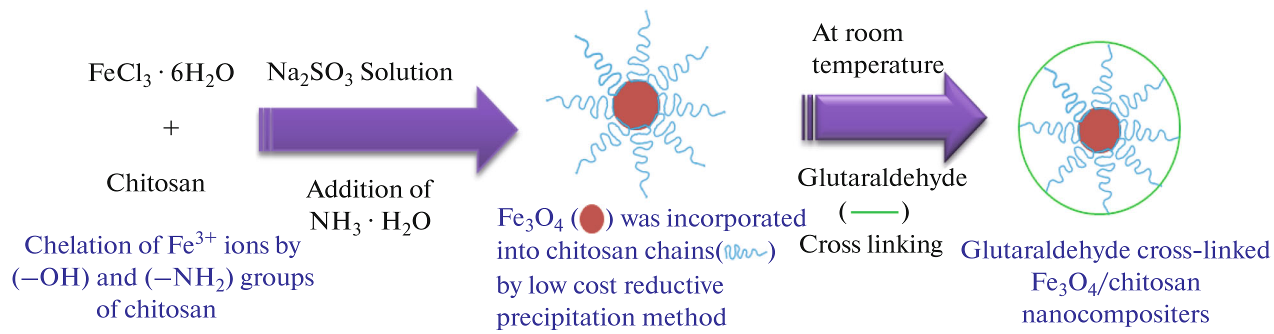

Fig. 2. Schematic representation of the synthesis of Fe_3O_4/chitosan nanocomposites.

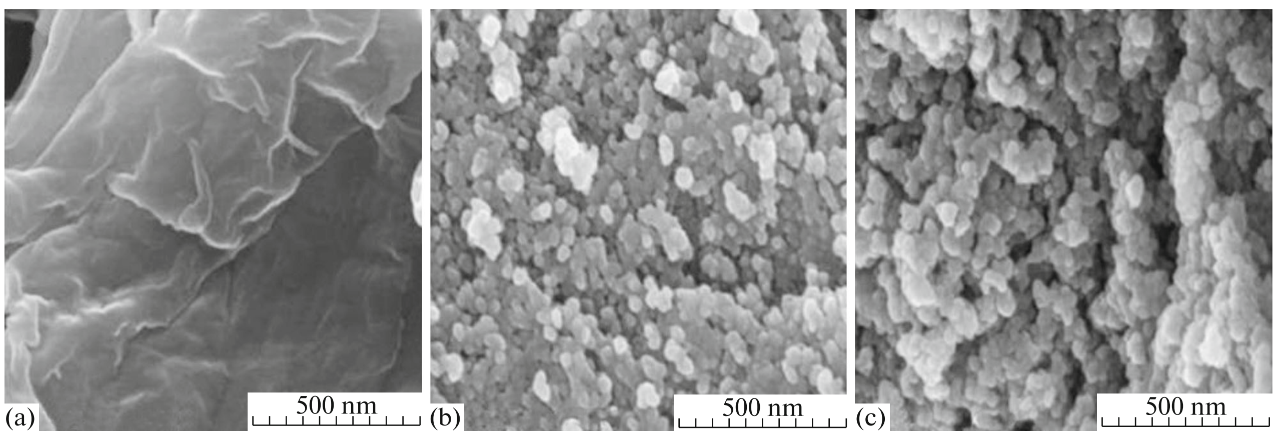

Fig. 3. FE-SEM analysis images: (a) chitosan, (b) Fe_3O_4 nanoparticles, and (c) Fe_3O_4/chitosan nanocomposites.

where, C_0 and C_e are respectively the initial and equilibrium concentration (mg/L) of the CR solution, W is the adsorbent weight in g, and V is the solution volume in liter(s). The removal ratio (R) for adsorption of CR on the Fe_3O_4/chitosan nanocomposites was calculated as a percentage using the following equation:

$$R(\%) = \frac{(C_0 - C_e)}{C_0} \times 100. \quad (2)$$

Adsorption isotherms were acquired for mixtures of 1 g/L of the Fe_3O_4/chitosan nanocomposites with CR solutions having concentrations ranging from 10 to 100 mg/L; the mixtures were shaken for 24 h at 140 rpm and 30°C.

RESULTS AND DISCUSSION

Synthesis and characterization of Fe_3O_4/chitosan nanocomposites. In this study, a cost effective method of reduction precipitation were applied for synthesis of the Fe_3O_4/chitosan nanocomposites [18]. Glutaraldehyde was used as a cross-linking agent instead of epoxy chloropropane in the synthesis process. Non-toxic nature of the cross-linking agent gave safe nanocomposites for water treatment. The detailed stratergy for the synthesis of Fe_3O_4/chitosan nanocomposites by reduction precipitation method is explained in Fig. 2.

The nanoscale structural morphology of the nanocomposites was analyzed by means of SEM. Figure 3 shows the FE-SEM microscopic images of chitosan, the Fe_3O_4 nanoparticles, and the Fe_3O_4/chitosan nanocomposite. The FE-SEM images of chitosan (Fig. 3a) show a planar, smooth surface comprising bio-polymer sheets, while the FE-SEM images of Fe_3O_4 (Fig. 3b) are characterized by irregular, round, and quasi-spherical structures. In comparison, the FE-SEM image of the Fe_3O_4/chitosan nanocomposites clearly showed that the particles had a uniform size with irregular, round, and quasi-spherical particles; the surface of these particles was smooth due to coating of chitosan over the Fe_3O_4 core (Fig. 3c). Similar surface structures of Fe_3O_4/chitosan nanomaterials have been previously observed by [19].

This result confirms successful formation of the Fe_3O_4/chitosan nanocomposites. The particle size of the nanomaterials in the FE-SEM images (Fig. 3) confirms the nanoscale nature of the synthesized Fe_3O_4/chitosan nanocomposites. The FT-IR spectra of chitosan and the Fe_3O_4/chitosan nanocomposites

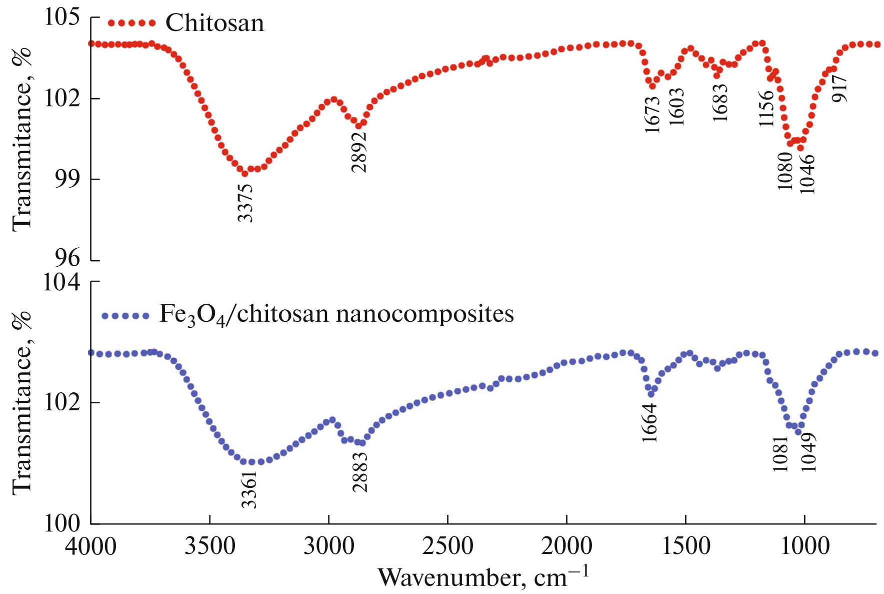

Fig. 4. FT-IR analysis of chitosan and Fe_3O_4/chitosan nanocomposites.

were analyzed in order to study their functional interactions. The FT-IR spectra displayed in Fig. 4, show absorption peaks of chitosan at 3375, 1673, 1603, and 1080 cm^{-1} that were attributed to the amino ($-NH_2$) and hydroxyl (–OH) groups, the C=O stretching vibration of the amide, the bending vibration of the ($-NH_2$) groups, and the C–O stretching vibration of C–OH, respectively [20, 21]. However, the FT-IR spectrum of the Fe_3O_4/chitosan nanoparticles showed absorption bands at 3361, 1664, and 1081 cm^{-1}, respectively, representing similar functional groups as observed in chitosan (Fig. 4). This result confirms the formation of nanocomposites comprising chitosan coated on Fe_3O_4 nanoparticles. A minor shift of the absorption peaks of chitosan was observed for the Fe_3O_4/chitosan nanoparticles, which is mainly due to complexation of Fe^{3+} with the amino and hydroxyl groups of chitosan [16].

The TGA data for chitosan, the Fe_3O_4 nanoparticles, and the Fe_3O_4/chitosan nanocomposites are presented in Fig. 5. The TGA curve of Fe_3O_4 showed a weight loss of 11% in the temperature range from room temperature to 200°C that is attributed to loss of residual water. The TGA curves of chitosan were characterized by a weight loss of 9.19% below 100°C and rapid weight loss between 250–500°C. These results are attributed to an initial weight loss due to the removal of physically adsorbed water and the subsequent weight loss is attributed to decomposition of pure chitosan. Similar results were obtained in thermogravimetric analysis of chitosan [22]. However, in the case of the Fe_3O_4/chitosan nanocomposites, three distinct stages of weight loss were observed in the TGA curve. An initial weight loss of about 11% was observed between room temperature and 100 °C, attributed to the evaporation of physically adsorbed water. The other two weight loss stages at 200–400 and 575–675°C were triggered by breakdown of the cross-linking chitosan in the Fe_3O_4/chitosan nanocomposites. From careful analysis of these results, it was concluded that the final temperature for breakdown of the Fe_3O_4/chitosan nanocomposites was higher than that of pure chitosan. During the reaction process, chitosan and Fe_3O_4 are linked together via chelation between chitosan (hydroxyl and amino groups) and Fe^{3+}, which ultimately causes conformational changes in chitosan, resulting in improved thermal stability of chitosan in the Fe_3O_4/chitosan nanocomposites. Similar TGA data were obtained by [18, 22].

Figure 6 shows a typical hyperstasis magnetic curve of Fe_3O_4/chitosan nanocomposites. Amost zero coercivity and remnance values were obtained in the magnetization curve, indicating supermagnetic properties of the synthesized nanocomposite. In addition, Fe_3O_4/chitosan nanocomposites gave the saturation magnetization of 21 emu/g. The synthesized magnetic nanocomposites were quickly attracted toward a magnet, and the reaction solution became clear. Thus, the Fe_3O_4/chitosan nanocomposites could be effectively collected from contaminated water by magnetic separation.

Adsorption of Congo red. Adsorption is an economic process for treatment of textile wastewater [4]. Various nano-adsorbents have recently been developed and applied to treatment of wastewater containing textile dye [23]. Chitosan polymers have been used for adsorption of CR [24]. Chitosan contains the amino functional group ($-NH_2$) and serves as an

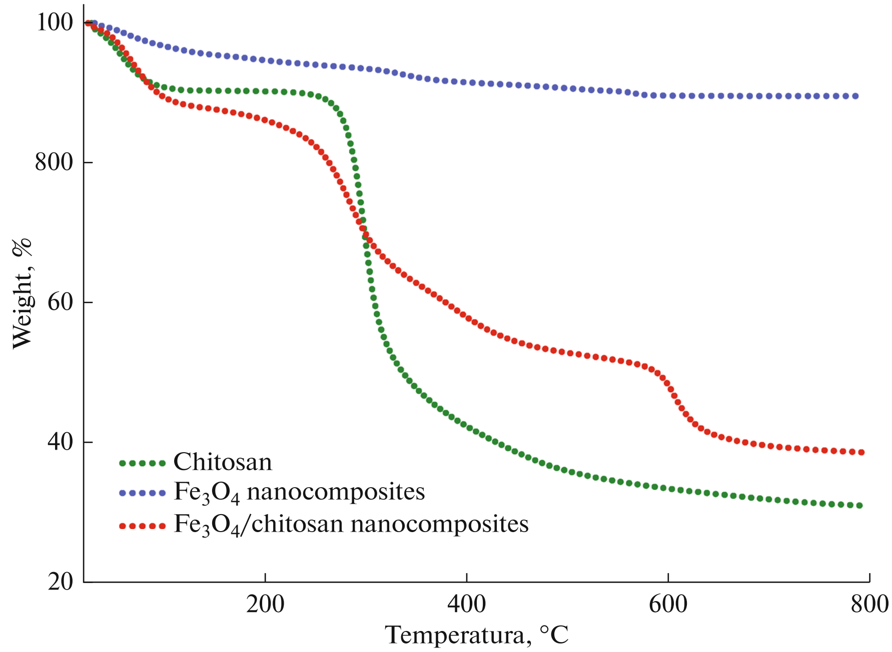

Fig. 5. TGA analysis of chitosan, Fe_3O_4 nanocomposites, and Fe_3O_4/chitosan nanocomposites.

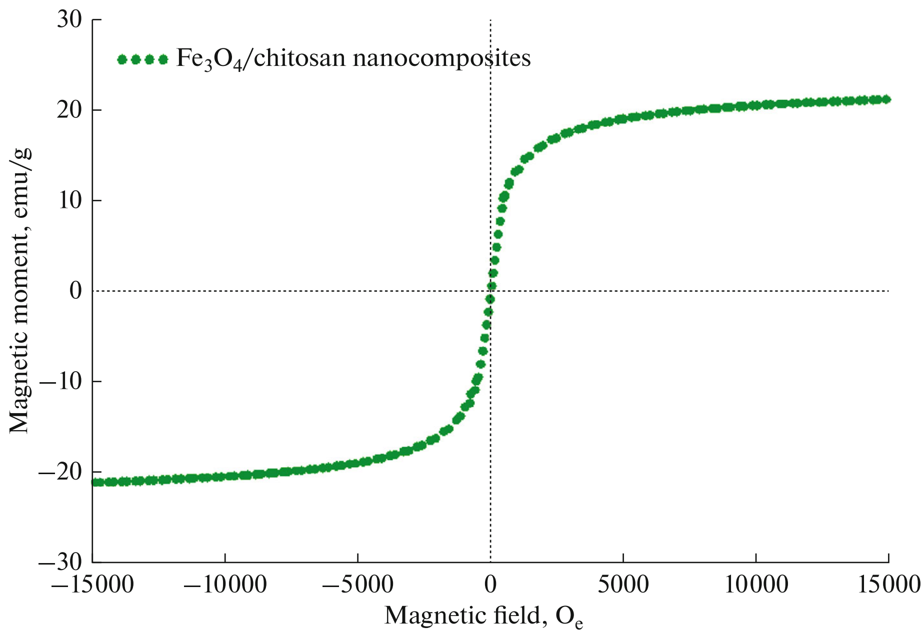

Fig. 6. MPMS analysis of Fe_3O_4/chitosan nanocomposites.

excellent adsorbent for anionic textile dyes [24]. Magnetically separable, inexpensive, highly efficient, and environment-friendly Fe_3O_4/chitosan nanocomposites offer better options for treatment of hazardous CR. In this study, 68% removal of CR was achieved with the developed Fe_3O_4/chitosan nanocomposites having magnetic properties. The UV-visible absorption spectra of CR before and after the adsorption treatment are presented in Fig. 7. The clearly observed decrease in the absorption intensity after treatment with the adsorbent provides evidence of the adsorption of CR on the Fe_3O_4/chitosan nanocomposites. The surface charge present on the Fe_3O_4/chitosan nanocomposites increases in acidic medium due to increased protonation of the amino groups, i.e., conversion of ($-NH_2$) to ($-NH_3^+$). The acidic CR dye contains negatively charged sulfonate groups ($-SO_3^-Na^+$).

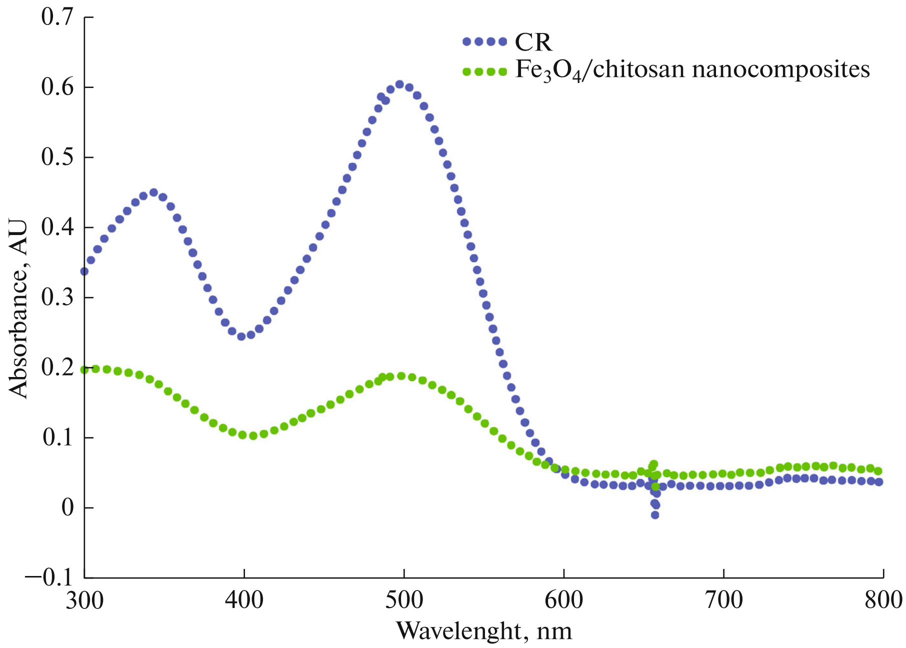

Fig. 7. UV-visible spectrophotometric analysis of control CR and Fe_3O_4/chitosan nanocomposites after adsorption.

Therefore, adsorption of CR on the Fe_3O_4/chitosan nanocomposites occurs via electrostatic attraction between the negatively charged dye molecules and positively charged amino groups of chitosan. The CR adsorption capacity of Fe_3O_4/chitosan nanocomposites in this study was compared with those obtained in previous studies of CR adsorption using different chitosan or magnetic adsorbents (Table 1). The adsorption capacity of the nanocomposites was higher than those of most of the adsorbents reported previously.

Equilibrium isotherm models such as Langmuir, Freundlich, and Tempkin were applied to the adsorption of CR on the Fe_3O_4/chitosan nanocomposites. The mechanism of the isothermal adsorption process was predicted by using the non-linear fitting method (OriginPro 8 software). The non-linear equations of the isotherm models were represented as Langmuir (Eq. (3)) [30], Freundlich (Eq. (4)) [31], and Tempkin (Eq. (5)) [32].

$$q_e = \frac{q_m K_a C_e}{1 + K_a C_e}, \tag{3}$$

$$q_e = K_F C_e^{\left(\frac{1}{n}\right)}, \tag{4}$$

$$q_e = \frac{RT}{b_T \ln(A_T C_e)}, \tag{5}$$

where, q_e is the adsorption capacity of the adsorbent at equilibrium (mg/g), C_e is the equilibrium concentration of CR in solution (mg/L), q_m is the mono-layer

Table 1. Comparative study of CR adsorption considering maximum adsorption capacity (q_{max})

Adsorbent	q_{max}, m/g	Reference
Fe_3O_4/chitosan nanocomposites	47.00	This study
Magnetic Fe_3O_4@graphene nanocomposite	33.66	[25]
Chitosan coated magnetic iron oxide	42.62	[26]
Cellulose/chitosan hydrogel beads	40.00	[27]
Magnetic core manganese oxide shell nanoparticles	42.00	[28]
Powdered Fe_2O_3	25.70	[29]
Hollow Zn–Fe_2O_4 nanospheres	16.10	[30]

adsorption capacity (mg/g), and K_a, K_F, n, A_T and b_T are the Langmuir, Freundlich, and Tempkin isotherm constants (Eqs. (3)–(5)). The Langmuir equation assumes that the adsorption process is monolayer in nature [33]. In comparison, the Freundlich isotherm empirical equation assumes a heterogeneous nature of the system [29]. The Tempkin model represent the hear of the adsorption [22]. Table 2 shows the correlation coefficients (r^2) for fitting of the Langmuir (r^2 = 0.993), Freundlich (r^2 = 0.935), and Tempkin (r^2 = 0.978) isotherm models. From these r^2 values, it was deduced that the data obtained from the experiments fit best to the Langmuir model. Figure 8a (Langmuir model), Fig. 8b (Freundlich model), and Fig. 8c (Tempkin model) show the experimental adsorption equilibrium; the fit of the empirical data to the isotherm models followed the order: Langmiur > Tempkin > Freundlich.

The separation factor, R_L, was calculated in order to evaluate the favorability of the adsorption process by using Eq. 6.

$$R_L = \frac{1}{1 + K_a C_0}, \quad (6)$$

Table 2. Different adsorption isotherm models and their obtained parameter values

Isotherm model	Parameters	Obtained values
Langmuir	q_m, mg/g	47.01
	K_L, L/mg	0.19
	r^2	0.993
Freundlich	K_F, mg/g	14.01
	n	3.37
	r^2	0.935
Tempkin	b_T	113.00
	A_T	2.18
	r^2	0.978

where R_L (the separation factor) is dimensionless and indicates the isotherm shape, C_0 is the initial CR concentration, and K_L is the obtained Langmuir constant. The R_L values provide an indicator of whether the adsorption process is (i) favorable (R_L < 1), (ii) unfavorable (R_L > 1), (iii) linear (R_L = 1), or (iv) irreversible (R_L = 0) [34] based on the isotherm data. The R_L

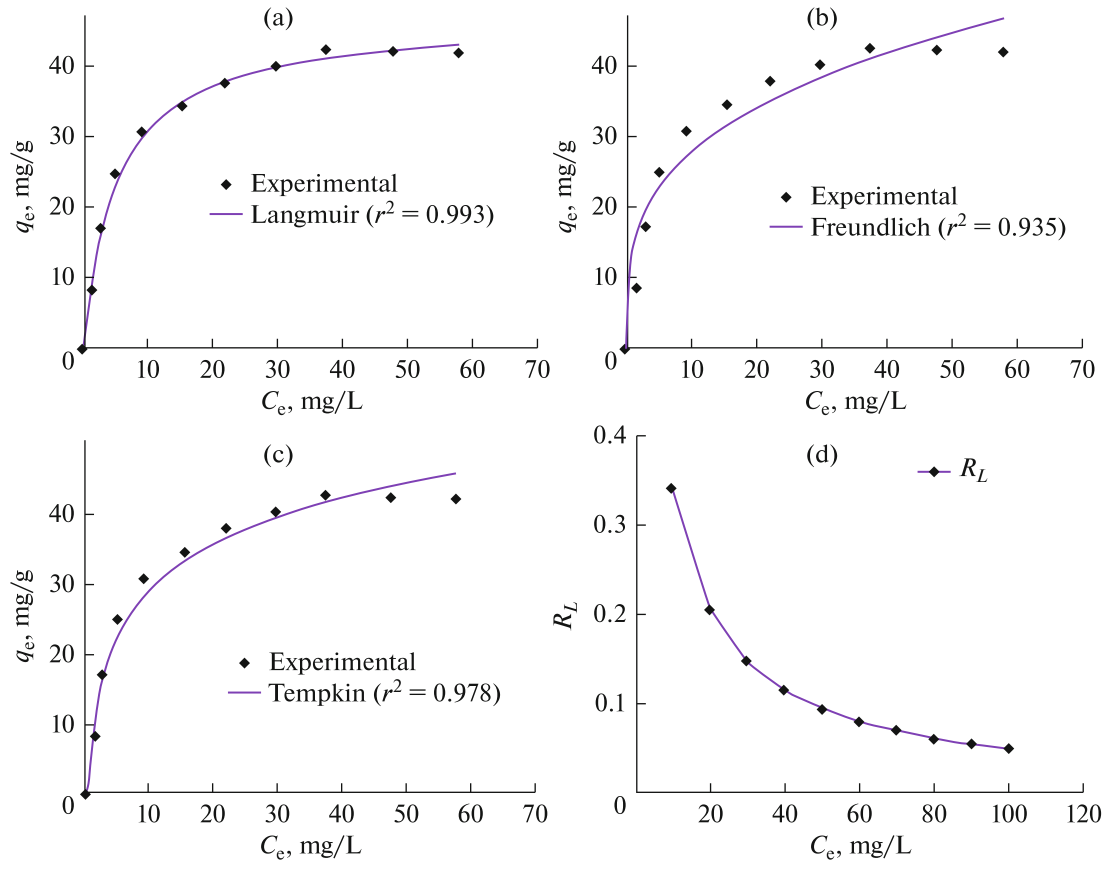

Fig. 8. Adsorption dynamics study: (a) Langmuir model, (b) Freundlich model, (c) Tempkin model, and (d) variation of separation factor RL at different initial CR concentrations.

value obtained for adsorption of CR on the Fe_3O_4/chitosan nanocomposites fell between 0 and 1 (Fig. 8d), indicating favorable adsorption dynamics.

CONCLUSIONS

Magnetic Fe_3O_4/chitosan nanocomposites were successfully synthesized by reduction precipitation. FE-SEM, FT-IR, and TGA analyses indicated successful coating of the adsorptive chitosan species on magnetic iron oxide (Fe_3O_4). The supermagnetic nature of Fe_3O_4/chitosan nanocomposites was confirmed by MPMS analysis. The Fe_3O_4/chitosan nanocomposites exhibited a good adsorptive removal capacity for CR. Adsorption isotherm analysis revealed that the Langmuir model provided a better fit of the data for this system than the Freundlich and Tempkin models. The obtained R_L factor suggests that CR adsorption on the nanocomposite is a favorable process. Therefore, inexpensive, magnetic, and efficient nanocomposites for adsorptive treatment of hazardous dye CR were successfully developed.

FUNDING

This research was supported by the Basic Science Research Program through the National Research Foundation of Korea (NRF) funded by the Ministry of Education (NRF-2018R1A6A1A03024962).

NOTATION

q_e	adsorption capacity of the adsorbent at equilibrium, mg/g
C_0	initial concentration of CR in solution before adsorption, mg/L
C_e	equilibrium concentration of CR in solution after adsorption, mg/L
q_m	mono-layer adsorption capacity, mg/g
K_a	Langmuir isotherm constant
K_F, n	Freundlich isotherm constants
A_T, b_T	Tempkin isotherm constants

REFERENCES

1. Elmoubarki, R., Mahjoubi, F.Z., Tounsadi, H., Moustadraf, J., Abdennouri, M., Zouhri, A., El Albani, A., and Barka, N., Adsorption of textile dyes on raw and decanted Moroccan clays: Kinetics, equilibrium and thermodynamics, *Water Resour. Ind.*, 2015, vol. 9, p. 16. https://doi.org/10.1016/j.wri.2014.11.001
2. Rasool, K., Woo, S.H., and Lee, D.S., Simultaneous removal of COD and Direct Red 80 in a mixed anaerobic sulfate-reducing bacteria culture, *Chem. Eng. J.*, 2013, vol. 223, p. 611. https://doi.org/10.1016/j.cej.2013.03.031
3. Afkhami, A. and Moosavi, R., Adsorptive removal of Congo red, a carcinogenic textile dye, from aqueous solutions by maghemite nanoparticles, *J. Hazard. Mater.*, 2010, vol. 174, p. 398.
4. Kadam, A.A., Kamatkar, J.D., Khandare, R.V., Jadhav, J.P., and Govindwar S.P., Solid-state fermentation: Tool for bioremediation of adsorbed textile dyestuff on distillery industry waste-yeast biomass using isolated *Bacillus cereus* strain EBT1, *Environ. Sci. Pollut. Res. Int.*, 2013, vol. 20, p. 1009.
5. Kadam, A.A., Jang, J., and Lee, D.S., Facile synthesis of pectin-stabilized magnetic graphene oxide Prussian blue nanocomposites for selective cesium removal from aqueous solution, *Bioresour. Technol.*, 2016, vol. 216, p. 391.
6. Gupta, V.K., Carrott, P.J.M., Ribeiro Carrott, M.M.L., and Suhas, Low-cost adsorbents: Growing approach to wastewater treatment—A review, *Crit. Rev. Environ. Sci. Technol.*, 2009, vol. 39, p. 783. https://doi.org/10.1080/10643380801977610
7. Rampino, A., Borgogna, M., Blasi, P., Bellich, B., and Cesàro, A., Chitosan nanoparticles: Preparation, size evolution and stability, *Int. J. Pharm.*, 2013, vol. 455, p. 219.
8. Tømmeraas, K., Köping-Höggård, M., Vårum, K.M., Christensen, B.E., Artursson, P., and Smidsrød, O., Preparation and characterisation of chitosans with oligosaccharide branches, *Carbohydr. Res.*, 2002, vol. 337, p. 2455.
9. Wang, J. and Chen, C., Chitosan-based biosorbents: Modification and application for biosorption of heavy metals and radionuclides, *Bioresour. Technol.*, 2014, vol. 160, p. 129.
10. Ambashta, R.D. and Sillanpää, M., Water purification using magnetic assistance: A review, *J. Hazard. Mater.*, 2010, vol. 180, p. 38.
11. Reddy, D.H.K. and Lee, S.M., Application of magnetic chitosan composites for the removal of toxic metal and dyes from aqueous solutions, *Adv. Colloid Interface Sci.*, 2013, vols. 201–202, p. 68.
12. Denkbas, E.B., Kilic, E., Birlikseven, C., and Ozturk, E., Magnetic chitosan microspheres: Preparation and characterization, *React. Funct. Polym.*, 2002, vol. 50, p. 225.
13. Yang, P.F. and Lee, C.K., Hyaluronic acid interaction with chitosan-conjugated magnetite particles and its purification, *Biochem. Eng. J.*, 2007, vol. 33, p. 284.
14. Singh, J., Srivastava, M., Dutta, J., and Dutta, P.K., Preparation and properties of hybrid monodispersed magnetic α-Fe_2O_3 based chitosan nanocomposite film for industrial and biomedical applications, *Int. J. Biol. Macromol.*, 2011, vol. 48, p. 170.
15. Dodi, G., Hritcu, D., Lisa, G., and Popa, M.I., Core–shell magnetic chitosan particles functionalized by grafting: Synthesis and characterization, *Chem. Eng. J.* 2012, vol. 203, p. 130.
16. Cao, C., Xiao, L., Liu, L., Zhu, H., Chen, C., and Gao, L., Visible-light photocatalytic decolorization of reactive brilliant red X-3B on Cu_2O/crosslinked-chitosan nanocomposites prepared via one step process, *Appl. Surf. Sci.*, 2013, vol. 271, p. 105.

17. Kadam, A.A. and Lee, D.S., Glutaraldehyde cross-linked magnetic chitosan nanocomposites: Reduction precipitation synthesis, characterization, and application for removal of hazardous textile dyes, *Bioresour. Technol.*, 2015, vol. 193, p. 563.

18. Cao, C., Xiao, L., Chen, C., Shi, X., Cao, Q., and Gao, L., In situ preparation of magnetic Fe_3O_4/chitosan nanoparticles via a novel reduction–precipitation method and their application in adsorption of reactive azo dye, *Powder Technol.*, 2014, vol. 260, p. 90.

19. Zhang, L., Zhu, X., Sun, H., Chi, G., Xu, J., and Sun, Y., Control synthesis of magnetic Fe_3O_4–chitosan nanoparticles under UV irradiation in aqueous system, *Curr. Appl. Phys.*, 2010, vol. 10, p. 828.

20. Chen, J.Y., Zhou, P.J., Li, J.L., and Li, S.Q., Depositing Cu_2O of different morphology on chitosan nanoparticles by an electrochemical method, *Carbohydr. Polym.*, 2007, vol. 67, p. 623.

21. Li, W., Xiao, L., and Qin, C., The characterization and thermal investigation of chitosan-Fe_3O_4 nanoparticles synthesized via a novel one-step modifying process, *J. Macromol. Sci. Part A.*, 2010, vol. 48, p. 57.

22. Zhu, H., Jiang, R., Xiao, L., Chang, Y., Guan, Y., and Li, X., Photocatalytic decolorization and degradation of Congo Red on innovative crosslinked chitosan/nano-CdS composite catalyst under visible light irradiation, *J. Hazard. Mater.*, 2009, vol. 169, p. 933.

23. Batool, S., Akib, S., Ahmad, M., Balkhair, K.S., and Ashraf, M.A., Study of modern nano enhanced techniques for removal of dyes and metals, *J. Nanomater.*, 2014, p. 1.

24. Chatterjee, S., Chatterjee, S., Chatterjee, B.P., and Guha, A.K., Adsorptive removal of congo red, a carcinogenic textile dye by chitosan hydrobeads: Binding mechanism, equilibrium and kinetics, *Colloids Surf., A,* 2007, vol. 299, p. 146.

25. Yao, Y., Miao, S., Liu, S., Ma, L.P., Sun, H., and Wang, S., Synthesis, characterization, and adsorption properties of magnetic Fe_3O_4@graphene nanocomposite, *Chem. Eng. J.,* 2012, vol. 184, p. 326.

26. Zhai, Y. Zhai, J. Zhou, M., and Dong, S., Ordered magnetic core–manganese oxide shell nanostructures and their application in water treatment, *J. Mater. Chem.*, 2009, vol. 19, p. 7030.

27. Li, M., Wang, Z., and Li, B., Adsorption behaviour of congo red by cellulose/chitosan hydrogel beads regenerated from ionic liquid, *Desalin. Water Treat.*, 2015, vol. 3994, p. 1.

28. Gonawala, K.H. and Mehta, M.J., Removal of color from different dye wastewater by using ferric oxide as an adsorbent, *J. Eng. Res. App.*, 2014, vol. 4, p. 102.

29. Rahimi, R., Kerdari, H., Rabbani, M., and Shafiee, M., Synthesis, characterization and adsorbing properties of hollow Zn–Fe_2O_4 nanospheres on removal of Congo red from aqueous solution, *Desalination*, 2011, vol. 280, p. 412.

30. Langmuir, I., The constitution and fundamental properties of solids and liquids, *J. Am. Chem. Soc.*, 1916, vol. 38, p. 2221.

31. Freundlich, H., Over the adsorption in solution, *J. Phys. Chem.*, 1906, vol. 57, p. 51.

32. Tempkin, M. and Pyzhev, V., Kinetics of ammonia synthesis on promoted iron catalyst, *Acta Phys. Chim. USSR.*, 1940, vol. 12, p. 327.

33. Zhu, H., Zhang, M., Liu, Y., Zhang, L., and Han, R., Study of congo red adsorption onto chitosan coated magnetic iron oxide in batch mode, *Desalin. Water Treat.*, 2012, vol. 37, p. 46. https://doi.org/10.1080/19443994.2012.661252

34. Debnath, S., Maity, A., and Pillay, K., Magnetic chitosan–GO nanocomposite: Synthesis, characterization and batch adsorber design for Cr(VI) removal, *J. Environ. Chem. Eng.*, 2014, vol. 2, p. 963.